SIMULATION ANALYSIS FOR INDOOR TEMPERATURE INCREASE AND REDUCTION OF HEATING LOAD IN THE DETACHED HOUSE WITH BUOYANCY VENTILATED WALL IN WINTER

Kan LIN[1], Shinsuke KATO[2]

1 Institute of Industrial Science,
The University of Tokyo
Room Cw403, Building of IIS, 4-6-1 Komaba,
Meguro-ku, Tokyo, 153-8505 Japan

2 Institute of Industrial Science,
The University of Tokyo
Room Cw403, Building of IIS, 4-6-1 Komaba,
Meguro-ku, Tokyo, 153-8505 Japan
**Corresponding author: kato@iis.u-tokyo.ac.jp*

ABSTRACT

Detached residential wooden houses are a common type of housing in Japan. Decay of wooden components within the walls is easily caused by condensation or defective flushing. To solve this problem, a double-skin system with a room-side air gap was developed. In this system, during winter, the airflow in the ventilated wall circulates freely around the whole house. Therefore, during daytime, the airflow moves solar heat to base, and releases heat to the house at night which can increase indoor temperature. The purpose of this study is to evaluate the flow rate in the ventilated wall and evaluate indoor temperature increase and reduction of heating load in winter. Therefore, it is important to develop an expression for flow rate in the wall. An airflow-energy simulation program was used to predict flow rates in the ventilated wall, and the performance of air-flows in several exterior walls of the house was investigated. The results verify that the flow rate in the ventilated walls increase with solar radiation. By using the double-skin system with a room-side air gap, the heating load in winter was reduced by 5%.

KEYWORDS

Double-skin system, Simulation, Buoyancy ventilation, Heating load, Reduction

INTRODUCTION

Wooden detached houses, which have wood-based structural insulation materials for walls and flooring, are widely used in Japan. However, many problems exist with this type of home construction. For example, during the summer period, incoming solar radiation is not equally distributed, leading to uneven indoor temperature distribution. In the winter period, indoor humidity is closely related to the durability of the building envelope. Moisture leaking from the interior rooms increases the risk of condensation on the walls, because the surface temperature of the wall is low. Condensation on the walls may cause the wood used in the houses' construction to decay. In addition to condensation from interior rooms, water vapour condenses on

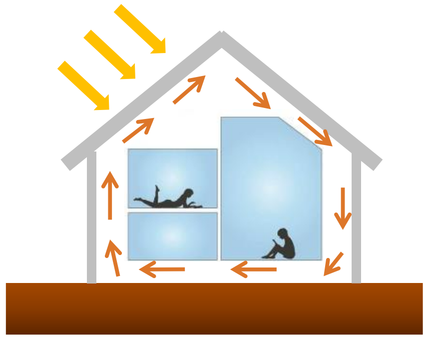

Figure 1: Double-skin system of room-side air gap with buoyancy ventilated wall applied to detached house in winter

wooden window frames, and rainwater can leak through the roof and walls. The increased moisture is absorbed by the wooden structure of the house, and reduces the endurance and strength of the wood, and also accelerates its decay.

To remove the moisture between the external and internal walls, a double-skin system is commonly installed to detached houses. A double-skin system consists of a multi-layered façade, with a buffer space used for ventilation. This system can integrate the mechanical ventilation with natural ventilation so that air can move freely in the buffer space.

In summer, air vents in the basement are opened and the ventilation fans on top of the roof are turned on to facilitate airflow through the ventilated wall, and out the roof. Airflow in the ventilated wall removes heat from solar radiation and from the internal wall. The airflow discharges heat in the wall and attic space, while obtaining cold heat from the ground under the floor. This ensures that the rooms are kept in moderate temperature and comfort.

In winter, the airflow in the ventilated wall circulates freely around the whole house. Therefore, during daytime, the airflow moves solar heat to base, and releases heat to the house at night which can increase indoor temperature.

Although houses using this system have been built for about 30 years in Japan, only a few studies have been conducted on them. Using a simulation of a model house from previous research, Ozaki et al. analyzed the airflow speed in the wall, as well as the airflow in the space under the floor during the summer period. However, there is hardly any information available regarding the actual airflow and thermal effects of this system. For this reason, it is difficult to select appropriate strategies to maintain airflow rate in the ventilated wall.

The objective of this study is to understand the basic properties of the double-skin system, temperature increase, and reduction in heating load during the summer period by performing a ventilation network simulation. To perform calculations during the winter period, we used a network simulation by creating two building models with spaces in the air gap and rooms of the house that were regarded as independent nodes. The impact of each element to the airflow rate was estimated, and the heating load reduction effect of the system was examined in the simulation.

The results show airflow rate and speed for each wall and reduction in the heating load when buoyancy ventilated wall was used to detached house. The reduction in the heating load increased significantly when buoyancy wall was used. In addition, natural indoor temperature increased slightly.

METHODOLOGIES

Simulation Software

To calculate the airflow in the buffer space, we used the variable energy calculation software TRNSYS17, and its add-on program TRNFlow. TRNFlow is designed based on COMIS3.1, a ventilation network calculation software, and can perform the iterative calculations by resolving the movement of the air and heat at the same time in TRNSYS.

Building Model

In this research, the house model (4th region) proposed by IBEC, Institute for Building Environment and Energy Conservation, as a standard detached house in Japan was used in the simulation. This house model is a two-story house with 120.07 m^2 total floor area, and it is intended for a four-person family. There are several spaces divided by rooms, as shown in figure 2. Occupants’ schedules as well as the lighting, equipment, ventilation, and air conditioning are based on the investigation. The dimensions and the basic configuration of the building were set based on this model. In addition, the dimensions of the air gap in the ventilated wall were set based on the real house.

The air gap in the ventilated wall is shown in figure 3. The area of the air gap in which air moves upwards is represented as the blue portion. Grooves are arranged on the surface of the insulation material in equal intervals. These create openings between the insulation and the other components, so that air flows freely. The air gap is divided into several zones by resistance parts, such as vents or these openings. In such zones, the flow path is narrower than the open air gap. For the calculations by TRNFlow, we modeled the air gap as an “airnode,” and defined any resistance parts as an “airlink.” For each airlink, the relationship of the mass flow rate and the pressure difference is calculated based on equation (1). In equation (1), a common formula for ventilation, the value of C_s, for each airlink, was decided by fixing α to 0.6 as a typical value. Also determined was the opening area A of the airlink, from the actual specification of this house. The value of n was determined to be 0.5, from the above substitution for the opening area, which is reflected in equation (2).

$$\dot{m} = C_s \cdot (\Delta p)^n \tag{1}$$

$$\dot{m} = \alpha A \sqrt{2\rho \cdot \Delta p} \tag{2}$$

$\dot{m}$: mass flow rate [kg / h], α: flow coefficient [-], A: opening area [m^2],
ρ: air density [kg/m^3] , Δp: pressure difference [Pa]

In this simulation, a simple building model that does not take into account the air infiltration, was used; neither air leaking into the rooms, nor outside air from the gas passage is considered. A simple network that connects the air gap to the outside air was created, as shown in figure 4.

With this model, it is possible to estimate the potential of the maximum amount of airflow generated by mechanical ventilation, regardless of the influence of air infiltration. On the other hand, because heat from solar radiation and internal heat cannot be discharged by infiltration, simulation results may show that the room temperature is higher than the actual environment.

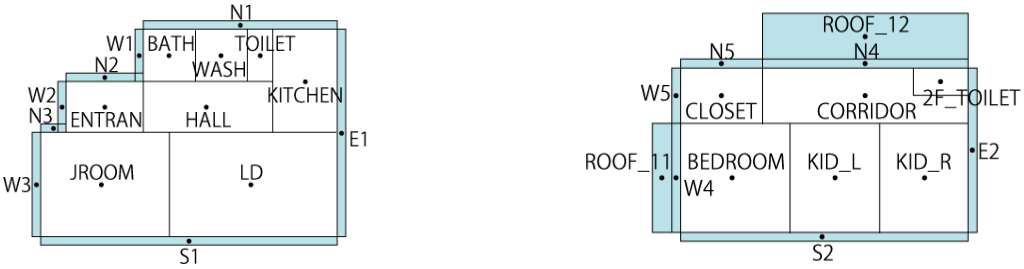

Figure 2: Zones and airnodes of the building model in TRNSYS

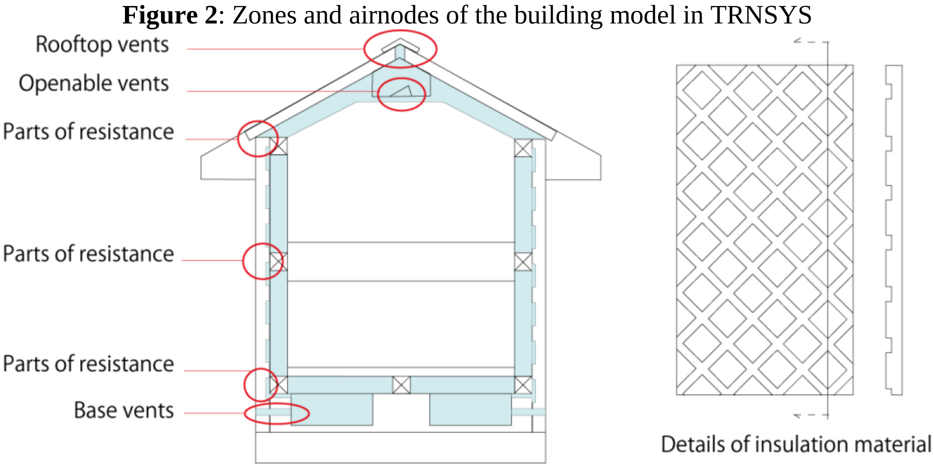

Figure 3: Overview of the air gap and insulation material

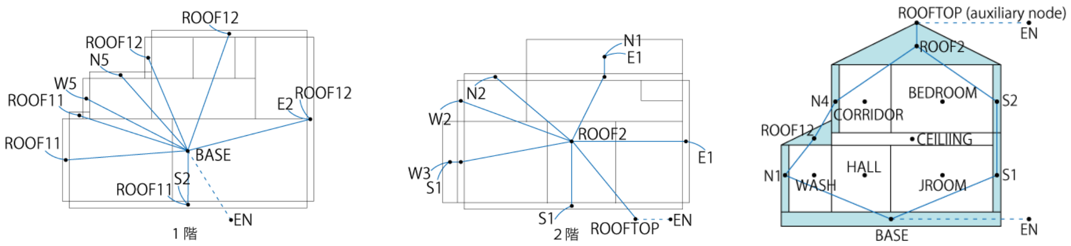

Figure 4 : Overview of airlinks in TRNFlow

Table 1: Building Properties

Wall of external side	Extruded polystyrene foam = 50 mm + Air layer = 15 mm + Tile = 10 mm
Wall of internal side	Gypsum board = 13 mm
Air gap thickness	120 mm
Roof	Extruded polystyrene foam = 50 mm + Air layer = 30 mm + Plywood = 10 mm + Slate = 5 mm
Base	EPS 50 mm + RC 150 mm + EPS 50 mm
Internal wall, Ceiling, Floor	U = 3.125 W/m^{2}K, 4.082 W/m^{2}K, 4.082 W/m^{2}K
Window, double-glazing	U = 1.8 W/m^{2}K, Shading coefficient = 0.5
Infiltration	None

Table 2: Ventilated Wall Setting

Opening area A [m^2]	Part of resistance in the air gap	0.00396 m^2/m (opening area per unit length wall)
	Ventilation unit at the rooftop to outside	0.0919
	Attic space to the ventilation unit at the rooftop	0.0755
	Outside to under-floor space	0.0720
Constants		α = 0.6, ρ = 1.2, n = 0.5

Table 3: Calculation Conditions

Internal heat gain	Exists (based on the schedule by IBEC)
Ventilation	None
Air-conditioning	None, Exists (based on the schedule by IBEC)
Ground temperature at 1m depth	9°C
Weather data	Expanded AMeDAS standard data (2000) , Tokyo
External wind	None
Calculation period	11/1 - 2/28 (plus 3 days for run-up period)

Calculation Conditions

The calculation conditions used in this study are listed in Table 1 through Table 4. Table 1 lists the properties of the walls, air gap, windows, etc. The conditions of the ventilated wall are listed in Table 2, and the calculation conditions are listed in Table 3. For evaluating the airflow rate and reduction effects, a case with buoyancy ventilated wall and a case without buoyancy ventilated wall are supposed.

To estimate the properties of airflow in the ventilated wall at natural room temperature, the simulation was first performed without air-conditioning. Then, calculations were carried out with air conditioning, and the effect of heating load reduction due to heat carried by airflow in the wall was estimated. The air-conditioning temperature was set to 20°C, and a total of five rooms—living room, kitchen, bedroom, and two children's rooms—were regarded as air-conditioned.

As shown in Table 3, the schedule of internal heat generation, ventilation, and air-conditioning was set according to the criteria of the IBEC standard. The ground temperature at 1m depth was set to 9°C, in reference to the results of past measurements. For weather data, including external wind, AMeDAS' expansion 2000 standard data in Tokyo was used. The calculation period was 11/1 - 2/28 (plus 3 days for run-up period) in the study.

RESULTS AND DISCUSSION

The temperature decrease during representative day is shown in Figure 5. Indoor temperature and the temperature of base change along with the variation of ambient temperature. The figure shows the average temperature of base is around 12°C when the ground temperature at 1m depth was set to 9°C.

Figure 6 shows the temperature decrease during representative day. The effect of the temperature decrease in 2 rooms is slight. The temperature in the living room increases by 0.3°C, when buoyancy ventilated wall is used. Temperature decrease in the bedroom is smaller than temperature decrease in the living room. This is because the heating schedule in the living room concentrates during the daytime while heating schedules of the bedroom concentrate in the nighttime.

Figure 7 shows flow rate for each wall during representative days, by direction. The figure shows both positive airflow and negative airflow in walls, and flow direction along a wall (upward direction) is considered positive. Based on the graph, the flow rate for each wall is affected by the outdoor temperature. The flow rates in the wall N1and N4 change drastically, and the biggest flow rate is as much as 2m^3/h. The flow rates in the walls N2, N3, and N5 are low when compared to the walls N1 and N4, which range from -0.5 to 0.5m^3/h. In east walls and south walls, all walls change drastically due to the influence of solar radiation during daytime. The biggest flow rate is as much as -2m^3/h, which range from -2 to 0.5m^3/h. In west walls, all walls change slightly because these walls are not seriously affected at solar radiation during daytime.

Figure 8 shows flow speed for each wall during representative days. The figure shows both positive airflow and negative airflow in walls, and flow direction along a wall (upward direction) is considered positive. Based on the graph, the flow rate for each wall is affected by the outdoor temperature. The flow rates in the wall N3and N5 change drastically. The flow speed in the walls N1, and N4 change gently when compared to the walls N3 and N5, which range from 1 to 2.5cm/s. In east walls and south walls, all walls change drastically due to the influence of solar radiation during daytime. The biggest flow rate is as much as 2cm/s, which range from -1 to 2cm/s.

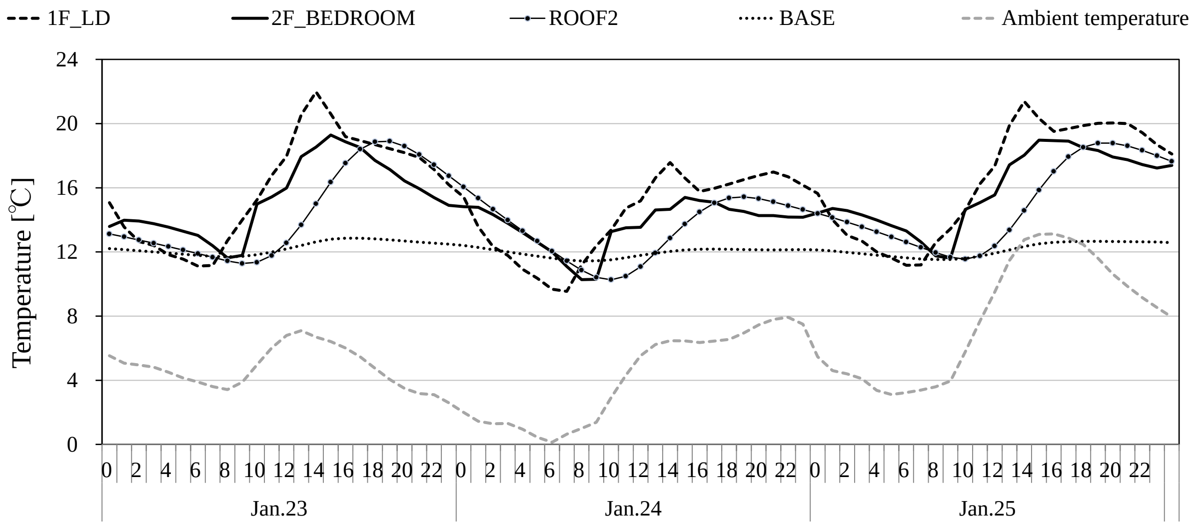

Figure 5: Temperature during representative days

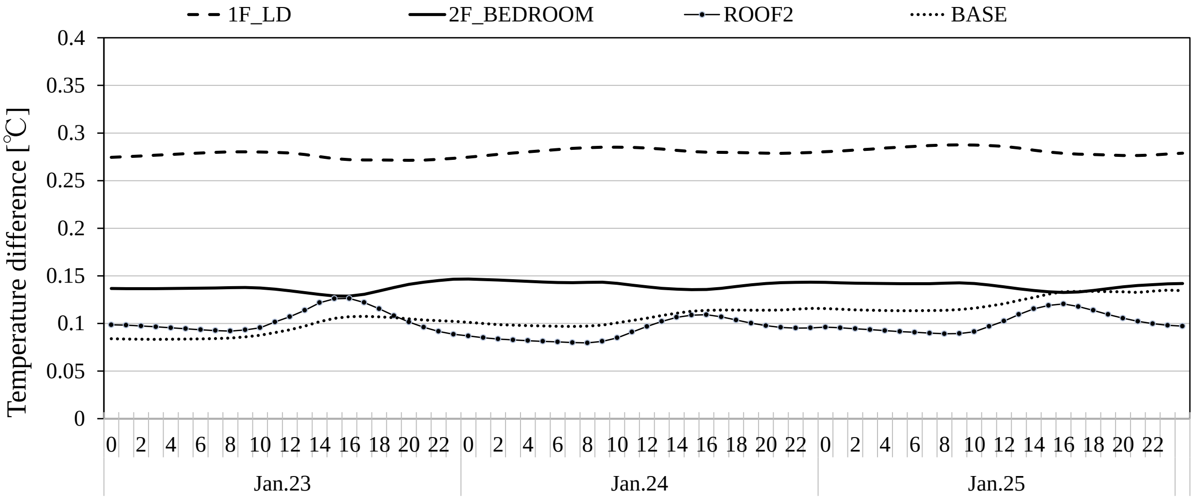

Figure 6: Temperature decrease during representative days

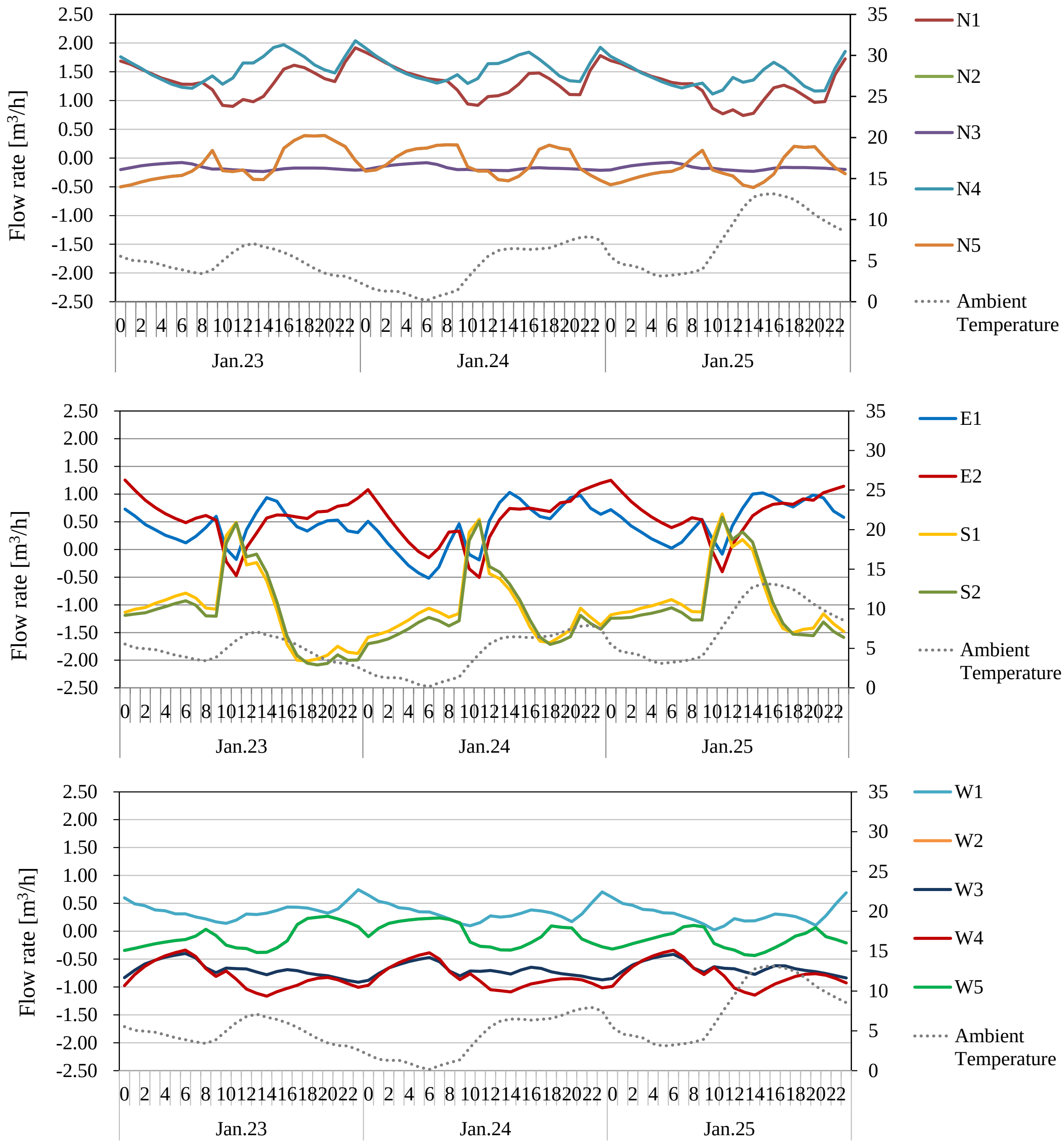

Figure 7: Flow rate for each wall during representative days

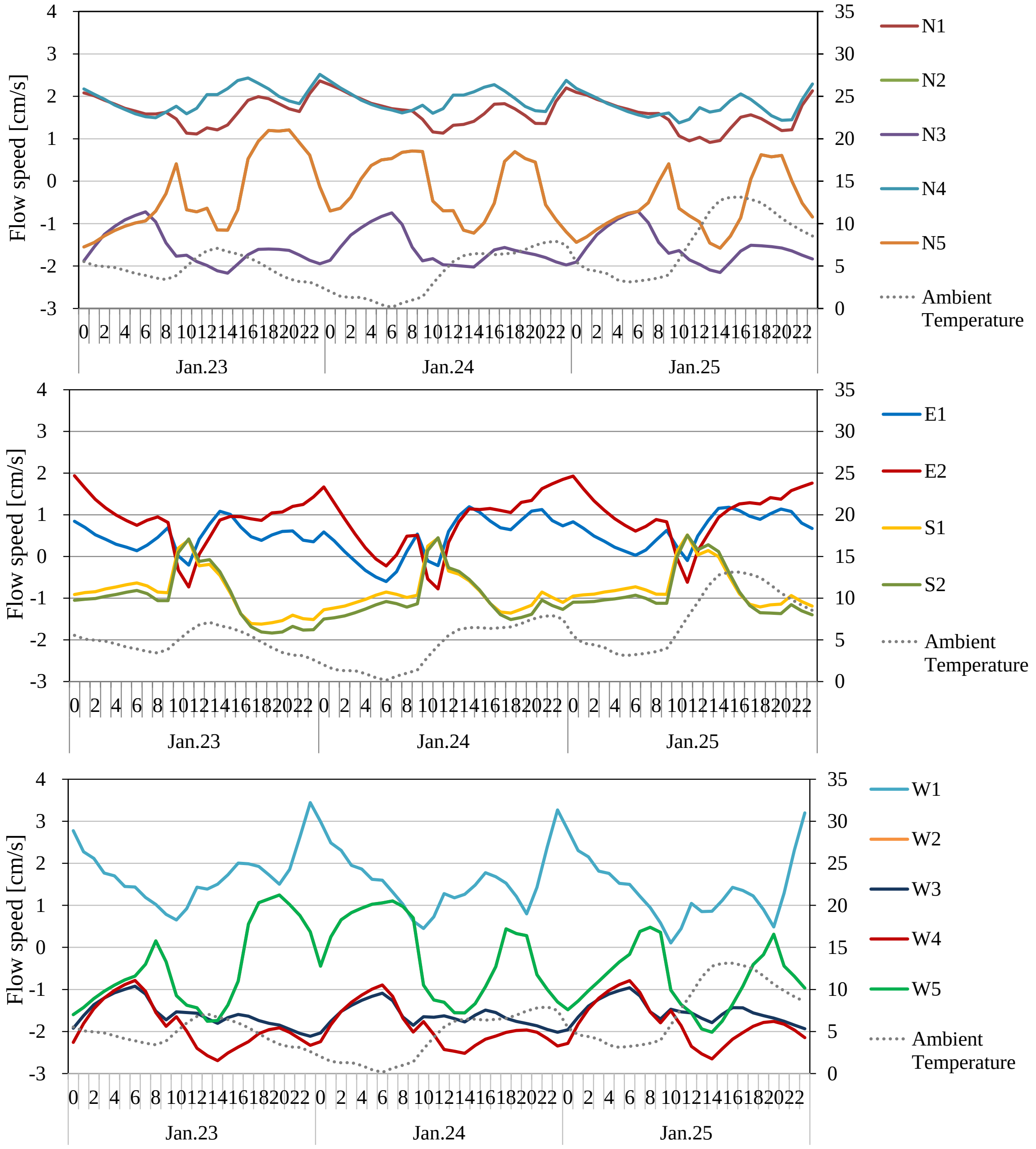

Figure 8: Flow speed for each wall during representative days

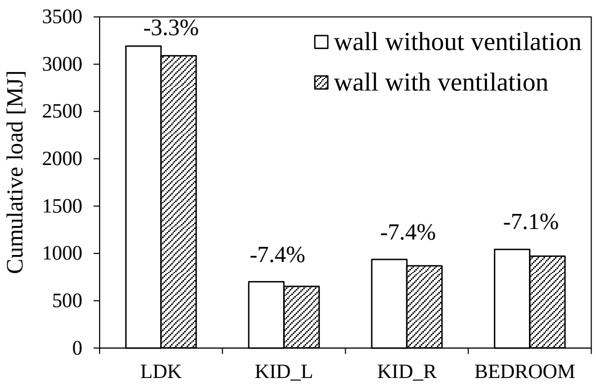

Figure 9: Total heating load in each room

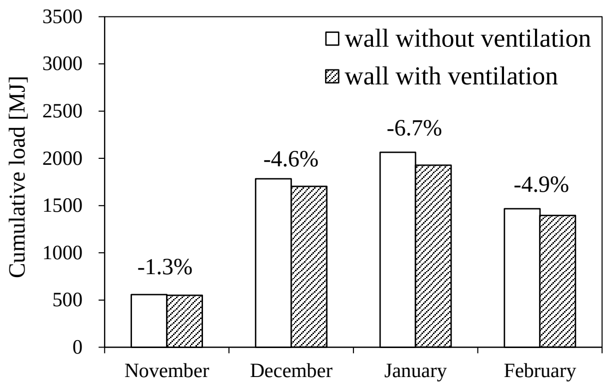

Figure 10: Total heating load in each month

Figure 9 shows the total heating load in the ventilated walls for each room, for the case with air-conditioning set at 20°C. Results for the four rooms are shown in the graph. The two children's rooms receive the largest heating load reduction because it consumes the least energy among the four rooms. The average heating load reduction for the dining room from June to September was reduced by 5.1%.

Figure 10 shows the total heating load from November to February for each month. The heating load during the period from November to February was reduced by 1.3%, 4.6%, 6.7%, and 4.9%, respectively. The reduction was largest in January in which the temperature was lowest.

CONCLUSIONS

In this study, we evaluated the airflow rate in the air gap of a double-skin system, the heating load reduction, and the temperature increase by performing a ventilation network simulation. The temperature in the living room increases by 0.3°C, when buoyancy ventilated wall is used. Temperature decrease in the bedroom is smaller than temperature decrease in the living room. This is because the heating schedule in the living room concentrates during the daytime while heating schedules of the bedroom concentrate in the nighttime.

In general, the average heating load reduction for the dining room from June to September was reduced by 5.1%. The two children's rooms receive the largest heating load reduction because it consumes the least energy among the four rooms. The heating load during the period from November to February was reduced by 1.3%, 4.6%, 6.7%, and 4.9%, respectively. The reduction was largest in January in which the temperature was lowest.

It was found that the total period heating load is reduced while the ventilated wall is working and the air-conditioning is on. It seems that this effect is mainly because the air-conditioning settling time was reduced by the room temperature increases. As a result, it is expected that the heating load supplied from subfloor ground surface Therefore, a further simulation of geothermal heat is necessary for future study. Furthermore, because heat from solar radiation and internal heat cannot be discharged by infiltration, the simulation result shows the room temperature is higher than that of the actual environment. To evaluate the influence of infiltration, a simulation that considers infiltration between the interior-exterior wall interface and the wall-room interface is needed in further research.

REFERENCES

Ozaki, A. (1992). Heat and water transfer through an ventilated structure using urethane panels [in Japanese]. *Summaries of technical papers of Annual Meeting Architectural Institute of Japan, D,* 945-946.

Institute for Building Environment and Energy Conservation. (2009). *Description of the energy consumption calculation method in the standards of judgment of the housing business building owners* [in Japanese].

Kurabuchi, T. (2009). Wind tunnel experiments on surface wind pressure and cross-ventilation flow rate in densely populated residential area: study on proper design method of locating windows aiming at utilization of cross-ventilation in densely populated residential area (part 1) [in Japanese]. *Journal of environmental engineering 74(642), 951-956*.